Electronic structure and total-energy calculations by a semi-self-consistent augmented-plane-wave method

M. A. Keegan
Computational Sciences and Informatics Institute, George Mason University, Fairfax, Virginia 22030

D. A. Papaconstantopoulos
Complex Systems Theory Branch, Naval Research Laboratory, Washington, D.C. 20375-5345
and Computational Sciences and Informatics Institute, George Mason University, Fairfax, Virginia 22030
(Received 31 August 1994)

We have adopted the Harris functional approximation in a standard framework of augmented-plane-wave (APW), density-functional calculations. Our implementation of the Harris approximation is based on a charge density from a self-consistent APW band-structure calculation for one lattice constant. This charge density is then frozen for calculation of the electronic structure and total energy at other lattice constants and for other crystal structures. The advantage of this approach over standard implementations of the Harris approximation is that our scheme computes the correct band structure as well as the correct total energy. We have applied this scheme to a wide variety of materials, ranging from transition metals to binary and ternary compounds. We present several examples and use these examples to motivate discussions of the scheme. Using this method, we have calculated total energies, equilibrium lattice constants, and bulk moduli which are in very good agreement with self-consistent results.

I. INTRODUCTION

Efforts to shortcut the computational complexity of self-consistency cycles in density-functional calculations began early in the development of electronic structure methods. In the 1960s the efficiency of the augmented-plane-wave[1] (APW) method was improved by introducing group theory. This allowed block diagonalization of the secular equation and a substantial reduction in computational time. In the 1980s, the number of iterations through the self-consistency cycle was reduced by applying Broyden's charge density mixing.[2] At the same time, Andersen *et al.*[3] developed a scheme, called the force theorem, to eliminate self-consistency cycles when moving from one crystal structure to another. This "frozen-potential" approach was successful in determining structural energy differences for metals in the transition series.[4] In the same spirit, Harris went directly to the density functional when he proposed an approximation for eliminating cycles for weakly interacting fragments.[5] The Harris functional approximation is well known as a scheme for eliminating the self-consistency cycle without significant loss of accuracy in the total energies. The Harris functional approximation to the density-functional theory amounts to a reformulation of the Hohenberg-Kohn-Sham total-energy expression. Since the time of Harris' original paper, the approximation technique has been applied in many molecular and solid-state total-energy calculations.

Applications of the Harris functional approximation within solid-state calculations have been primarily associated with the linearized muffin-tin orbitals (LMTO) method and tight-binding formalisms. Polatoglou and Methfessel[6] showed the versatility and accuracy of the approximation with applications to *sp*- and *d*-bonded metals, covalently bonded semiconductor Si, and for the ionicly bonded NaCl by calculating the cohesive energies, lattice constants, and bulk moduli. Soon after this, Polatoglou and Methfessel used the scheme in calculation of elastic moduli and vibrational properties, further demonstrating the accuracy of this approximation.[7] More recently, Methfessel and Schilfgaarde have derived a very simple expression for the force theorem based on the Harris total energy.[8] The Harris functional approximation has been used in surface and vacancy formation calculations, for example, by Finnis for Al systems.[9] The variety of these studies has provided a basis of understanding and demonstrates the applicability of the approximation. In addition, these studies have considered several variations to the proposal of Harris and have discussed the heuristics and systematics of different implementations of the approximation.

A systematic study of the Harris functional approximation in the first-row transition metal series was conducted by Paxton *et al.*[10]. Paxton *et al.* employed a highly accurate implementation of the full potential LMTO and concluded that "the Harris functional approximation is capable of reproducing very accurately the self-consistent calculations of static structural properties of transition metals."[10]

A weakness of the Harris functional scheme was pointed out by Read and Needs[11] and by Finnis.[9] In calculations of the surface energy in Al, the overlapped free atomic charge density was not smooth enough and overly extended. Finnis indicated that the Harris functional calculations required a renormalization of the free

atomic charge density in a way that applies a cutoff to the tail while conserving the total charge in order to obtain results within reasonable error of the self-consistent results. However, the renormalization involves a free parameter, which is nontransferable.

We have introduced a modification to the Harris functional approximation into a standard framework of APW calculations. These calculations are scalar relativistic within the local-density approximation[12](LDA). The difference in our implementation is that we perform one self-consistent calculation at one lattice constant and then we use the resulting charge density for "one shot" calculations at other volumes and structures. This has the advantage that energy bands and density of states are calculated accurately for all lattice constants and in other structures in addition to the total energy. This is not the case in the standard Harris approximation, which gives the wrong band structure.[6]

II. SEMI-SELF-CONSISTENT CALCULATIONS

In this section we describe the specifics of our method, which we name the semi-self-consistent (SSC) method. In the calculations discussed in this paper we have employed the muffin-tin approximation (MTA) with touching spheres. For cubic materials, the MTA gives results that are very close to those of full-potential methods. Also, we have tested our SSC approach for full-potential calculations in Pd and found that our methodology works well with the full potential, also.[13] We recall the following expression for the total energy due to Janak,[14]

$$E=\sum\epsilon_i+\int\rho_{\rm out}(r)V_{\rm in}[r]dr-2\mathcal{Z}\int\rho_{\rm out}(r)r^{-1}dr +2\int_0^{R_s}\rho_{\rm out}(r)r^{-1}dr\int\rho_{\rm out}(r')dr'+E_{\rm xc}+E_{\rm Mad}, \quad (1)$$

where ϵ_i are calculated one electron eigenvalues, $V_{\rm in}[r]$ is the input crystal potential, and $\rho_{\rm out}$ is the output charge density computed from the sum of squares of the wave functions. $E_{\rm xc}$ is the exchange and correlation energy calculated within LDA and $E_{\rm Mad}$ is the Madelung energy.

In the spirit of the Harris functional method, we have developed the procedure outlined in the following steps.

(1) For a given system we perform, by the APW method, a fully self-consistent calculation for one volume only.

(2) We use the self-consistent electron charge density resulting from the above calculation and solve Poisson's equation to generate Kohn-Sham local-density potentials at other volumes or for other structures.

(3) Using the potentials of step 2, we calculate the sum of the eigenvalues by the APW method without iterating.

(4) We compute the total energy of the system using the sums of eigenvalues from step 3, and for the other terms in Eq. (1) the self-consistent charge density of step 1 and the potentials of step 2.

We require the self-consistent charge density, $\rho_{\rm sc}$ at sufficient number of points in the numerical radial mesh to accommodate the largest volume desired for the set of total-energy calculations. In practice, we have found very good results by freezing a charge density larger than the LDA equilibrium lattice constant.

It should be clear that we have borrowed the idea of freezing the charge density from the Harris functional scheme, but our frozen charge density is self-consistent for one lattice constant. Furthermore, this should distinguish our implementation from the self-consistent atomic fragment method, proposed by Averill and Painter,[15] which prescribes an iterative scheme for updating the expansion coefficients of the basis functions using the Harris functional expression.

We have implemented this methodology to handle monatomic, diatomic, and large systems both accurately and with reduced computational complexity. Furthermore, our method yields accurate energy bands and density of states, which cannot be obtained using overlapping atomic charge densities, in the Harris scheme.

III. RESULTS

We have applied the formalism described in the previous section to a variety of materials. As examples, we present results from transition metals Ti, Cu, Nb, Rh, Ta, and Pt, transition metal monocarbides VC and FeC, and two supercell calculations for the ternary compounds, Al_4Cu_3Fe and $Al_{11}Cu_3Fe_2$. We have systematically calculated the total energy as a function of the volume, which allows computation of the equilibrium lattice parameter and bulk modulus. These properties are computed by fitting the energy data to the Birch model equation of state.[16] Properties computed in this work may be compared to the fully self-consistent calculations of Sigalas *et al.*,[17] which were performed within the same APW method as our semi-self-consistent calculations.

A. Transition metals

We demonstrate the essential advantage of the SSC scheme over the usual implementation of the Harris functional scheme by plotting the energy bands of Cu in the fcc structure. In this case, we have performed a SC calculation for lattice constant 6.85 a.u.; the resulting charge density is frozen for the SSC calculation. Figure 1 shows (a) the SSC energy bands, (b) the fully self-consistent energy bands, and (c) the Harris functional energy bands, all for the same lattice constant, $a = 6.65$ a.u. Note the discrepancies between the Harris functional energy bands and the fully self-consistent bands; most notably the crossing of the Cu $3d$ band and the Fermi level near X, which amounts to a severe distortion of the Fermi surface in the Harris functional results. The SSC bands are in very good agreement with the fully self-consistent bands.

As an additional demonstration of the quality of the SSC energy bands, we have calculated the occupied band width ($E_F - \Gamma_1$) and a measure of the d-bandwidth ($\Gamma_{12} - \Gamma'_{25}$). These quantities are plotted as a function of the lattice constant in Fig. 2(a) and Fig. 2(b), respectively. Note the overestimation of the bandwidths by the usual implementation of the Harris functional scheme and the good agreement between the SSC and SC re-

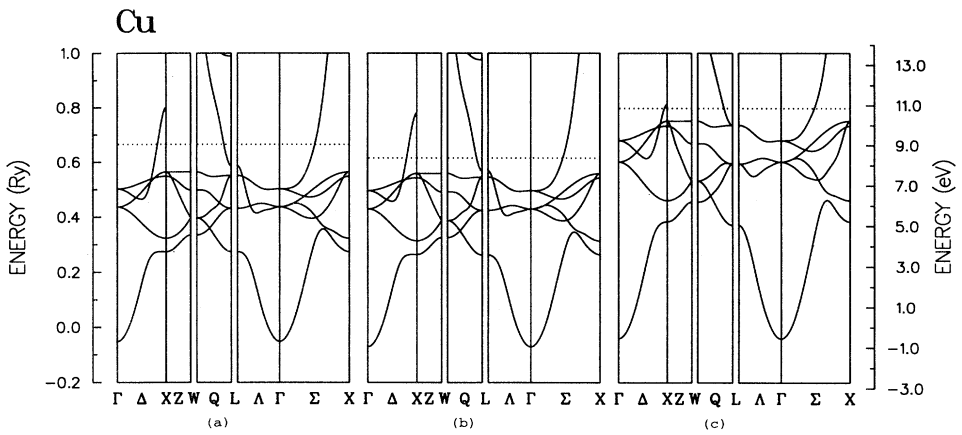

FIG. 1. Comparison of energy bands calculated in three computational methods for Cu(fcc). The method presented in this publication, the semi-self-consistent method, produced (a), which is in very good agreement with the fully self-consistent results (b). The third set of bands results from a standard implementation of the Harris approximation (c), the bands differ significantly.

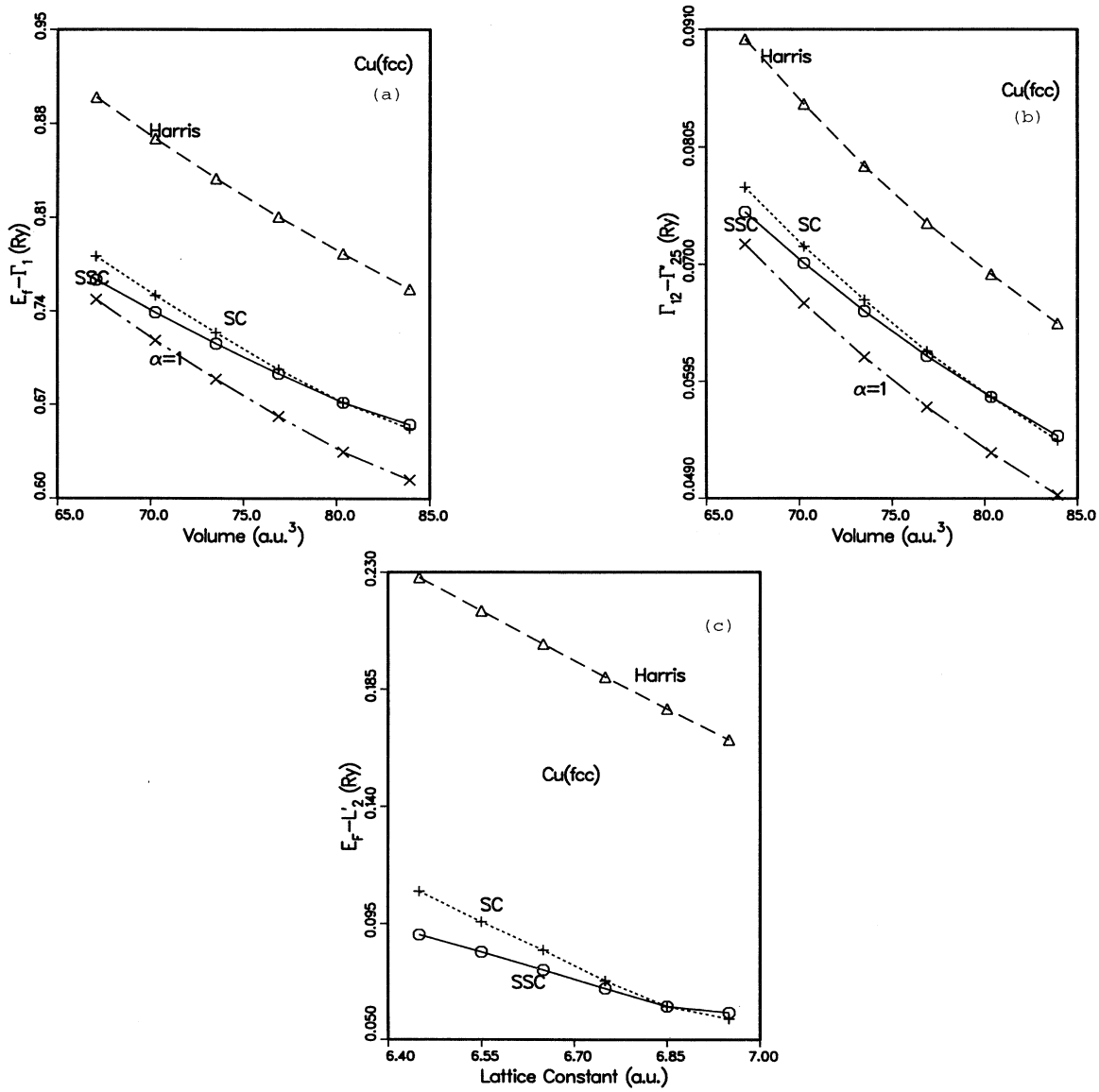

FIG. 2. Additional measures of the quality of the energy bands generated in three computational methods for Cu(fcc). The figure shows three different measures: (a) the occupied bandwidth ($E_F - \Gamma_1$), (b) a measure of the d-bandwidth ($\Gamma_{12} - \Gamma'_{25}$) and (c) a measure of the position of p levels ($E_F - L'_2$). In each case, the semi-self-consistent results (SSC) are in good agreement with the self-consistent results (SC), while the results from the standard implementation of Harris approximation is in poor agreement.

sults. A fourth curve appears in these figures: This is the occupied bandwidth and $\Gamma_{12} - \Gamma'_{25}$ calculated by the non-self-consistent Matheiss prescription with full Slater exchange correlation ($\alpha = 1$). As is well known, the $\alpha = 1$ is in good agreement with the SC energy bands for monatomic materials, but the total energy does not show similar agreement. A final indication of the quality of the band structure from the SSC calculation is taken from the plot of $E_F - L'_2$ shown in Fig. 2(c), which determines the position of a p-like level. Again we show a close agreement between SSC and SC results.

Next, we would like to show that we have achieved agreement with SC LDA calculations in total energies by comparing equilibrium lattice constants and bulk moduli calculated in the three methods: (1) SSC, (2) SC, and (3) the usual implementation of the Harris functional approximation (denoted "Harris"). Figure 3(a) shows the SSC and Harris equilibrium lattice constants plotted for several of the example materials on the y-axis ordinate versus the SC-LDA result for the same material on the x-axis ordinate. This means that a data point falling directly on the dashed line is in exact agreement with the SC-LDA results. Figure 3(b) shows the bulk moduli plotted in a similar way for the three methods. A more

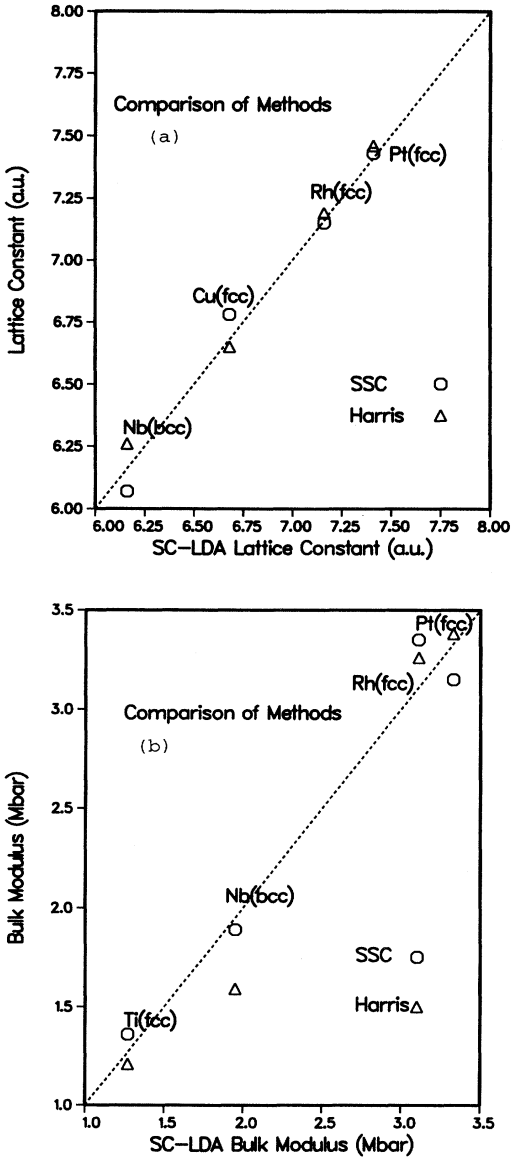

FIG. 3. Comparison of (a) theoretical equilibrium lattice constants and (b) theoretical bulk moduli from three computational methods. Results are shown for several transition metals.

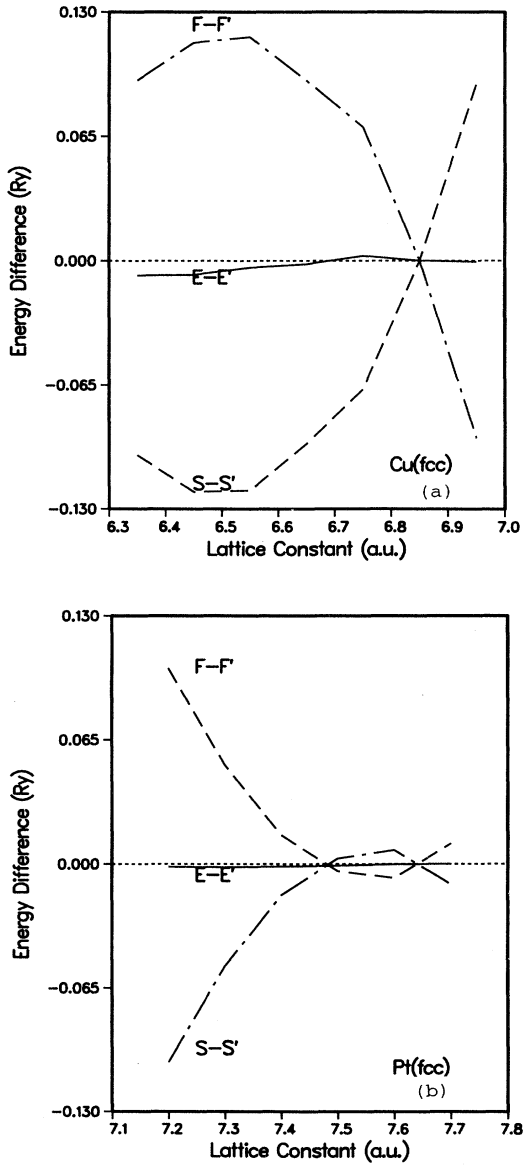

FIG. 4. A simple representation of error cancellations in the various terms of the total-energy expression of the semi-self-consistent and the self-consistent methods, for (a) Cu(fcc) and (b) Pt(fcc). Errors in the sum of eigenvalues ($S - S'$) term cencel errors in the remaining terms ($F - F'$) leading to a very small error in the total energy ($E - E'$).

TABLE I. Theoretical equilibrium lattice constants (a_o), bulk moduli (B_o), and structural energy differences($\Delta E_{\text{fcc}-\text{bcc}}$) calculated in three different schemes decribed in the text.

	a_o (a.u.)			B_o (Mbar)			$\Delta E_{\text{fcc}-\text{bcc}}$ (mRy)		
Element	SSC	SC	Harris	SSC	SC	Harris	SSC	SC	Harris
Ti	7.47	7.56	7.58	1.36	1.27	1.21	0.5	1.8	1.1
Cu	6.74	6.68	6.65	1.97	1.99	2.25	5.4	5.6	6.2
Nb	6.07	6.16	6.26	1.89	1.95	1.59	-31.9	-27.6	-26.9
Rh	7.15	7.16	7.19	3.35	3.11	3.26	31.8	33.0	38.1
Ta	6.09	6.22	6.21	1.93	2.00	2.15	-28.9	-25.7	-25.9
Pt	7.43	7.41	7.46	3.15	3.33	3.38	12.6	17.7	15.3

quantitative assessment can be made from Table I, which tabulates the results plotted in Figs. 3(a) and (b). The error in the SSC calculated lattice constant is less than 2% and the error in the SSC calculated bulk moduli is less than 8% when compared with the SC values. The bulk moduli reported are calculated at the theoretical minima of the respective curves.

In addition to tabulating the information plotted in Fig. 3, Table I provides the structural energy differences calculated in the three methods. This quantity is very sensitive, but is calculated correctly in all the test cases by each method. We are mostly concerned with the sign of this quantity, but the table demonstrates that the sign and magnitude of the energy difference is in good agreement with the self-consistent results. The conclusion that can be drawn from Table I is that the usual implementation of the Harris approach and our SSC method give results of similar accuracy for equilibrium lattice constants and for structural energy differences.

Finally, we have tried to understand the SSC method from a simple analysis of the error in the SSC total energy. Our analysis compares the difference of the total energy calculated in the SSC scheme E' and the total energy of the SC calculations E. We have separated the total energy into two terms: the sum of eigenvalues S and a term F, which includes all the other terms in Eq. (1) besides the sum of eigenvalues. Then for each volume of SC calculations, we perform the corresponding SSC calculation using the frozen charge density from a single SC calculation. The energy terms, separated as indicated, are compared at each volume in turn. We have plotted in Fig. 4(a) and (b) two curves as functions of the lattice constant representing the simple error in the SSC total-enegy terms. These two curves are the differences between the sum of eigenvalues term from the SC and SSC schemes (labeled $S - S'$ in the figure) and differences of remaining terms from the two methods (labeled $F - F'$ in the figure) for Cu and Pt in the fcc structure. The differences indicate a cancellation of errors from the sum of the eigenvalues term and the other terms leading to an overall good agreement in the total energy. The error in the SSC total energy is shown as the solid curve in Fig. 4(a) and (b) (labeled $E - E'$). This comparison should not be considered in terms of an absolute reference of energy because it severely confuses the simplistic intent of the analysis. In fact, as shown by Lambrecht *et al.*,[18] there is no meaningful absolute reference level.

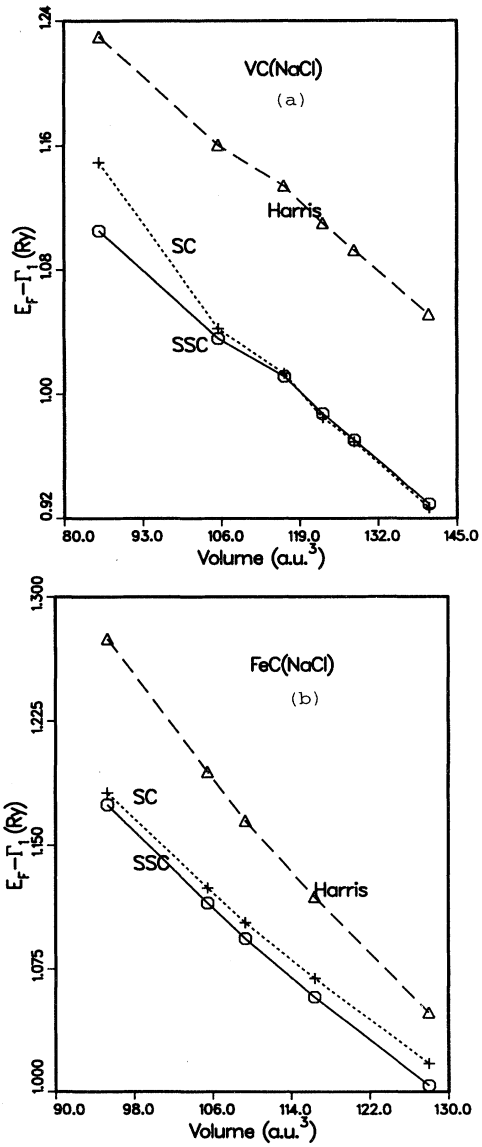

FIG. 5. Comparisons of occupied bandwidths ($E_F - \Gamma_1$) computed in three computational schemes for (a) VC(NaCl) and (b) FeC(NaCl). Results obtained in the semi-self-consistent method are in better agreement with self-consistent results than results obtained in the standard implementation of the Harris approximation.

TABLE II. Theoretical equilibrium lattice constants (a_o) and bulk moduli (B_o) calculated according to three different schemes decribed in the text.

	a_o (a.u.)			B_o (Mbar)		
Compound	SSC	SC	Harris	SSC	SC	Harris
VC	7.77	7.89	7.89	2.78	3.32	3.69
FeC	7.42	7.58	7.49	2.75	3.31	3.58

However, the energy shift will be the same for the sum of eigenvalues term and the remaining terms; thus, the cancellation of error in these terms is still valid.

B. Transition metal carbides

As an example of the capabilities of the SSC method to calculate correctly quantities of interest in compounds, we have calculated the total energy and bulk modulus for FeC and VC in the NaCl structure. We have performed these calculations according to three methods: (1) SSC, (2) SC, and (3) the Harris functional approximation. For FeC, we perform the SSC calculations using the charge density from the SC calculation at $a = 8.0$ a.u. For VC, we use the SC charge density, obtained at $a = 7.9$ a.u., in the SSC calculations. In both cases, the self-consistent calculations were performed for the compound, not for the components of the compound separately. As in the case of the transition metals, we find much better agreement between the energy bands of the SSC calculation and SC calculation than between the Harris functional calculation and the SC calculation. In this case, we have plotted the occupied bandwidth for both materials from the three calculational schemes. Figure 5(a) shows the occupied bandwidth ($E_F - \Gamma_1$) for VC and Fig. 5(b) for FeC. In both Figs. 5(a) and (b), the Harris functional approximation (denoted Harris) overestimates the occupied bandwidth, while the SSC results agree very well with the SC results. Results for calculations of the equilibrium lattice constant and bulk moduli are summarized in Table II for VC and FeC. The error in the equilibrium lattice constants versus the SC results is less than 2.5% and the error in the bulk moduli is less than 17%. It is clear from Table II that despite doing poorly in the band structure, the Harris functional method does get the lattice constant and bulk modulus correct and, in these two cases, is slightly better than the SSC method.

C. Ternary compounds

Finally, we would like to demonstrate the capability to calculate properties of large systems with the SSC scheme. We have calculated total energies and bulk moduli for two ternary systems. The first is Al_4Cu_3Fe in a bcc 8-atom supercell, using the SC charge density corresponding to lattice constant 11.2 a.u. And the other is $Al_{11}Cu_3Fe_2$ in a simple cubic 16-atom supercell, using the SC charge density corresponding to lattice constant 11.4 a.u. We have not included any spin polarization for Fe in our calculations. There is justification for this from Fe^{57} Mossbauer studies performed by Stadnik *et al.*,[20] which showed that Fe atoms bear no magnetic moment down to 1.5 K, for alloys in the same system with similar stoichiometries. In Fig. 6(a) and (b), the total energy as a function of lattice constant is plotted for Al_4Cu_3Fe and $Al_{11}Cu_3Fe_2$, respectively. Also indicated in Fig. 6 is the theoretical equilibrium lattice constant and bulk modulus. For the 8-atom Al_4Cu_3Fe, the SSC scheme finds 11.05 a.u. for the lattice constant compared with 10.93 a.u. calculated self-consistently; for the bulk modulus, the SSC scheme finds 1.63 Mbar slightly larger than the SC result of 1.55 Mbar. For the 16-atom $Al_{11}Cu_3Fe_2$, the

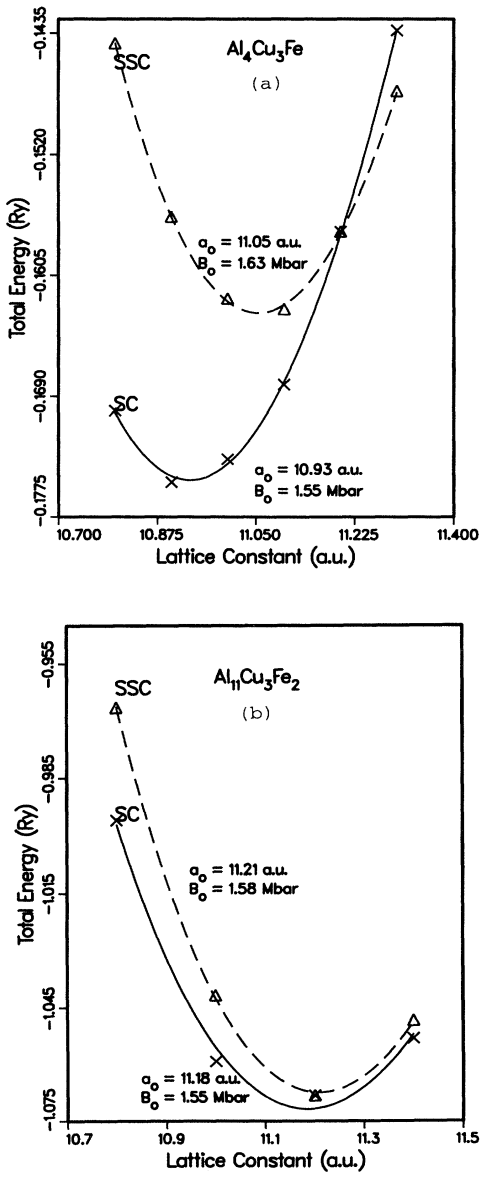

FIG. 6. Comparison of semi-self-consistent and self-consistent total-energy results for ternary compounds (a) Al_4Cu_3Fe and (b) $Al_{11}Cu_3Fe_2$.

lattice constant calculated in the SSC method is 11.21 a.u. which is in very good agreement with the SC result of 11.18 a.u.; the bulk modulus found in the SSC scheme is 1.58 Mbar in very good agreement with the 1.55 Mbar calculated self-consistently. We have calculated the occupied bandwidth ($E_F - \Gamma_1$) for these two materials according to both calculational schemes. This quantity is plotted in Fig. 7(a) for Al_4Cu_3Fe and for $Al_{11}Cu_3Fe_2$ in Fig. 7(b).

Self-consistent band structures and density of states (DOS) have been reported for these two stoichiometries,[20] these results may be compared to the SSC results presented in this paper. For Al_4Cu_3Fe, the DOS and energy bands are shown in Figs. 8(a) and 8(b), respectively. Figure 8(a) shows the total DOS (top panel), as calculated in the SSC method. The curves correspond to the lattice constant 11.10 a.u., the lattice constant nearest to the theoretically determined equilibrium. The lower panels of Fig. 8(a) show the angular momentum, site decomposed DOS useful for identifying the origin of the peaks in the total DOS. In Fig. 8(b), the energy bands are plotted along symmetry lines in the irreducible 1/48th of the bcc Brillouin zone. The flat Cu d levels are sandwiched above by the split Fe d levels and below by

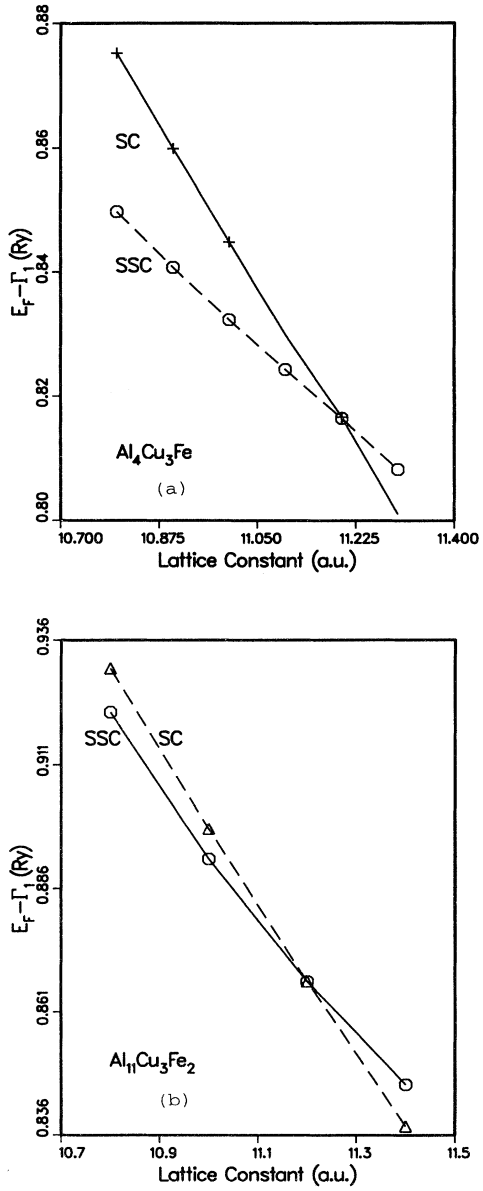

FIG. 7. Comparison of semi-self-consistent and self-consistent occupied bandwidths ($E_F - \Gamma_1$) for ternary compound (a) Al_4Cu_3Fe and (b) $Al_{11}Cu_3Fe_2$.

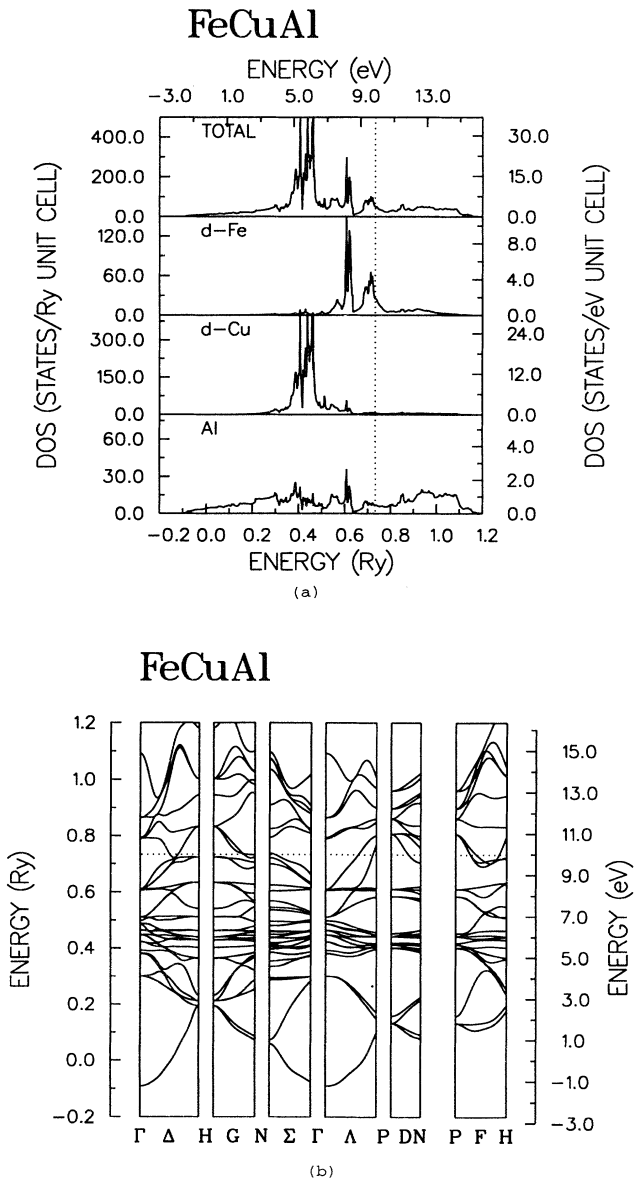

FIG. 8. Semi-self-consistent results for ternary compound Al_4Cu_3Fe. The figure shows (a) the density of states and (b) the energy bands.

the hybridized Al levels. For the 16-atom $Al_{11}Cu_3Fe_2$, the DOS and energy bands are shown in Figs. 9(a) and 9(b), respectively. These curves correspond to lattice constant 11.20 a.u., very close to the calculated equilibrium. In Fig. 9(a), the total DOS of states and several angular momentum, site decomposed DOS are plotted in the same manner as Fig. 8(a). Finally, Fig. 9(b) shows the energy levels along the symmetry lines of the simple cubic Brillouin zone. Above the flat Cu d levels are the Fe d levels, which show a different characteristic than in the Al_4Cu_3Fe material.

The computational complexity of these APW calculations is proportional to the number of atoms in the unit cell. To perform these calculations more efficiently, we have block diagonalized the secular equation using the group symmetry of the cubic supercells. However, even using group theory, the computer time requirements make self-consistent calculations too costly. So, our SSC scheme has huge gains over self-consistent calculations in supercell. For the 8-atom supercell, the SC calculation requires $\tau = 1800s$ per iteration. The number of iterations to reach self-consistency is $\sigma = 15$ and the number of lattice constants is $N_{\rm lat} = 6$ in order to accurately fit to the model equation of state. That means the total time used in the self-consistent calculation is

$$T_{\rm sc} = N_{\rm lat}\sigma\tau = 45 \text{ workstation hours.} \tag{2}$$

The SSC scheme requires self-consistent calculation at one volume plus $(N_{\rm lat}-1)$ calculations of the one electron energy levels at $\tau' = 1000s$ per lattice constant. Then the total time is

$$T_{\rm ssc} = \sigma\tau + (N_{\rm lat}-1)\tau' = 9 \text{ workstation hours} = \frac{1}{5}T_{\rm sc}. \tag{3}$$

The quantity τ' indicates the reduction in computational time enabled by the elimination of the input and output of wave functions. For the 16-atom supercell, SC calculations require $\tau = 4800s$ per iteration, now $T_{\rm sc}$ is 120 workstation hours. The SSC calculations are performed in $\tau' = 4000s$ for each of the additional volumes and a total time $T_{\rm ssc}$ 25 hs. In other words, properties that require about one week to be calculated self-consistently are being calculated in the span of a single day. We have approximated the time for a SC calculation of a 32-atom supercell to be on the order of three months, while the SSC calculation would require about three weeks.

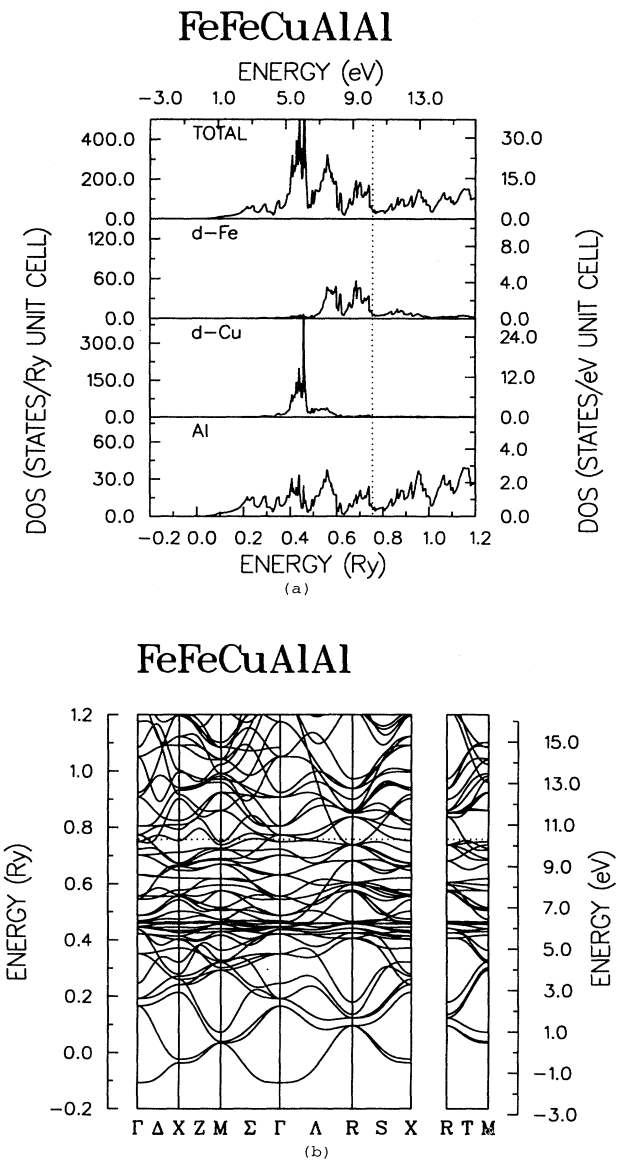

FIG. 9. Semi-self-consistent results for ternary compound $Al_{11}Cu_3Fe_2$. The figure shows (a) the density of states and (b) the energy bands.

IV. CONCLUSIONS

The usual implementation of the Harris functional approximation utilizes overlapping atomic charge densities. This implementation works well for obtaining equilibrium volumes and bulk moduli, but fails in the description of the energy bands or density of states. We proposed a method that freezes the charge density at its self-consistent value for one volume and carry out calculations in the spirit of the Harris functional approximation for other volumes and in different structures. We call this approach the SSC scheme and we have shown that it works as well as the usual implementation of the Harris method for the total energy, but it gives, in addition, the band structure very accurately. This SSC method is particularly advantageous for calculations of very large systems, where the fully self-consistent procedure is not practical.

ACKNOWLEDGMENTS

We wish to thank M. J. Mehl, W. E. Pickett, D. J. Singh, and A. C. Switendick for many helpful discussions and suggestions. This work was supported in part by the U.S. Office of Naval Research.

[1]J. C. Slater, Phys. Rev. **51**, 846 (1937); L. F. Mattheiss, J. H. Wood, and A. C. Switendick, in *Methods in Computational Physics*, 8th ed., edited by B. Alder, S. Fernbach, and M. Rotenberg (Academic, New York, 1968).
[2]C. G. Broyden, Math. Comput. **19**, 577 (1965); G. P. Srivastava, J. Phys. A **17**, L317-L321 (1984).
[3]O. K. Andersen, H. L. Skriver, H. Nohl, and B. Johansson, Pure Appl. Chem. **52**, 93 (1979).
[4]H. L. Skriver, Phys. Rev. B **31**, 1909 (1984).
[5]J. Harris, Phys. Rev. B **31**, 1770 (1985).
[6]H. M. Polatoglou and M. Methfessel, Phys. Rev. B **37**, 10 403 (1988).
[7]H. M. Polatoglou and M. Methfessel, Phys. Rev. B **41**, 5898 (1990).
[8]M. Methfessel and M. van Schilfgaarde, Phys. Rev. B **48**, 4937 (1993).
[9]M. W. Finnis, J. Phys. Condens. Matter **2**, 331 (1990).
[10]A. T. Paxton, M. Methfessel, and H. M. Polatoglou, Phys. Rev. B **41**, 8127 (1990).
[11]A. J. Read and R. J. Needs, J. Phys. Condens. Matter **1**, 7565 (1989).
[12]L. Hedin and B. I. Lundqvist, J. Phys. C **4**, 2064 (1971).
[13]D. A. Papaconstantopoulos and D. J. Singh, in *Statics and Dynamics of Alloy Phase Transformations*, edited P. E. A. Turchi and A. Gonis (Plenum Press, New York, 1994), p. 439–442.
[14]J. F. Janak, Phys. Rev. B **9**, 3985 (1974).
[15]F. W. Averill and G. S. Painter, Phys. Rev. B **41**, 10 344 (1990).
[16]F. Birch, J. Geophys. Res. **83**, 1257 (1978).
[17]M. Sigalas, D. A. Papaconstantopoulos, and N. C. Bacalis, Phys. Rev. B **45**, 5777 (1992).
[18]W. R. L. Lambrecht, B. Segall, and O. K. Andersen, Phys. Rev. B **41**, 2813 (1990).
[19]Z. M. Stadnik, G. Stroink, H. Ma, and G. Williams, Phys. Rev. B **39**, 9797 (1989).
[20]G. T. de Laissardiere, Z. Dankhazi, E. Belin, A. Sadoc, N. M. Duc, D. Mayou, M. A. Keegan, and D. A. Papaconstantopoulos (unpublished).